Rare Metal Materials and Engineering
Volume 49, Issue 1, January 2020
Available online at www.rmme.ac.cn

Science Press

Cite this article as: Rare Metal Materials and Engineering, 2020, 49(1): 0048-0058.

ARTICLE

Preparation of Low-sulphur Molybdenum Oxide by Microwave-activated Pre-calcination of Molybdenite

Wang Miao[1,2], Yang Shuangping[1,2], Guo Shuanquan[1], Cao Shuanwei[1], He Kai[3]

[1] Xi'an University of Architecture and Technology, Xi'an 710055, China; [2] Research Center of Metallurgical Engineering and Technology of Shaanxi Province, Xi'an 710055, China; [3] Jinduicheng Molybdenum Co., Ltd, Xi'an 710077, China

Abstract: Effect of microwave power, irradiation time and mass quantity on molybdenite activation desulfurization after microwave-activated pre-calcination treatment was studied; unreacted shrinkage nucleus model of gas-solid heterogeneous reaction was adopted to study reaction kinetics. Results show that molybdenite concentrate can absorb microwave well, and optimum desulfurization effect is obtained with 0.64 kW microwave irradiation of 30 g molybdenite for 6 min, and the relative sulphur content was reduced by 65.47% in contrast with traditional oxidizing roasting; the oxidation of molybdenite is a highly exothermic reaction with a faster oxidation rate at higher temperatures; the conversion rate is obviously increased at 540~630 ℃ with interfacial chemical reaction as a rate controlling step. The effect of microwave activation prior to conventional oxidative roasting was tested and verified. As for industrial applications, a short-time activated calcination pretreatment can be used to assist conventional oxidative roasting.

Key words: molybdenite; microwave activation; activated pre-calcination; low-sulphur molybdenum oxide; unreacted shrinkage nucleus model

Molybdenum resources in China account for 25% of the world's total reserves [1-3], of which about 99% exists as molybdenite [4]. Traditional hydrometallurgy extraction process is constrained by leaching costs and equipment problems [5-16]; pyrometallurgical process is usually preceded by oxidative roasting, desulfurization and conversion to molybdenum trioxide followed by ammonia leaching, while problems such as recovery rate, environmental pollution, and poor economic benefit of off-gas acid production exist [17-19]. Residual sulphur content of molybdenum trioxide (molybdenum calcine) is a key evaluation index that affects subsequent molybdenum yield and quality of various products [20].

Conventional heating transfers heat from the hotter external region to the cooler internal region by radiation, conduction and convection. The heating rate between various minerals is basically the same and temperature difference between each component is not obvious. Microwave heating depends on the direct absorption of electromagnetic energy by materials and heat is generated within it. Heat transfer takes place from the hotter core to the cooler surfaces [21]. Due to the selective heating of microwaves and the effective generation of heat inside the material [22,23], different components can be effectively dissociated at lower temperatures and react faster at higher temperatures. Therefore, microwave heating finds applications in various fields due to its high heating rates, reduced processing time and significant energy saving, and has been widely used for auxiliary crushing, leaching, roasting, drying, heat reduction, and impurity removal [24-34].

In order to solve the problems of difficulty in temperature control and sinterability, and poor oxidation performance in molybdenite roasting by traditional multi-hearth furnaces, the emphasis of this study is the novel application of molybdenite microwave pretreatment. The effects of conventional oxidative roasting and microwave

Received date: January 17, 2019
Foundation item: Shaanxi Science and Technology Coordination Innovation Project Plan (2015KTZDGY09-01); Shaanxi Provincial Department of Education Special Scientific Research Project (17JK0439); Xi'an University of Architecture and Technology Youth Science and Technology Fund (QN1316)
Corresponding Author: Yang Shuangping, Ph. D., Professor, School of Metallurgical Engineering, Xi'an University of Architecture and Technology, Xi'an 710055, P. R. China, Tel: 0086-29-82202923, E-mail: wmxauat@163.com

pre-calcination for molybdenum desulphurization treatment were comparatively studied, and the "activation" effect was verified.

1 Experiment

Molybdenite used in the experiment was gray lead color and metallic luster (chemical composition is presented in Table 1).

Molybdenum content was 52.21 wt% and sulphur content was 34.83 wt%, and gangue components were SiO_2, CaO, MgO and Cu, Pb, etc. It can be seen from XRD pattern in Fig.1 that molybdenum mainly exists in the form of MoS_2, and the crystal lattice is a standard layered structure[35-37] (SEM image and structural diagram in Fig.1) with complete dissociated surface, similar to the morphology of graphite which has distinct lamellar, scaly, and finely dispersed particles, and the particle size is in the range of tens to hundreds of microns.

Microwave activated roasting experiments were performed in the equipment (MKX-R1C1C microwave chemical synthesizer, Fig.2). N_2 was used as shielding gas. After activation pretreatment, the sample was roasted in a high temperature resistance furnace at 600 ℃ for 2 h with a heating rate from 10 K/min to 30 K/min. The inactivated route only adopts a high temperature resistance furnace as comparison, and the sample No. is M-0 in the following paper. STA409PC integrated thermal analyzer produced by German Chico was adopted for TG/DSC analysis. The calcination effect was characterized by the residual sulphur content (measured by carbon-sulphur analyzer) and effective oxidation rate.

For the reaction kinetic analysis, the dried molybdenite sample was heated from room temperature to 700 ℃ in air at heating rates of 5, 10, and 15 K/min. The effective oxidation rate of molybdenite was described by the ratio of the molybdenum content in molybdenum calcine to the total molybdenum content in molybdenite.

Table 1 Chemical composition of molybdenite (wt%)

Mo	S	Cu	Pb	WO_3	Bi	C	K	Fe	SiO_2	CaO	MgO
52.21	34.83	0.11	0.09	0.10	0.05	0.40	0.09	0.33	5.20	1.70	4.89

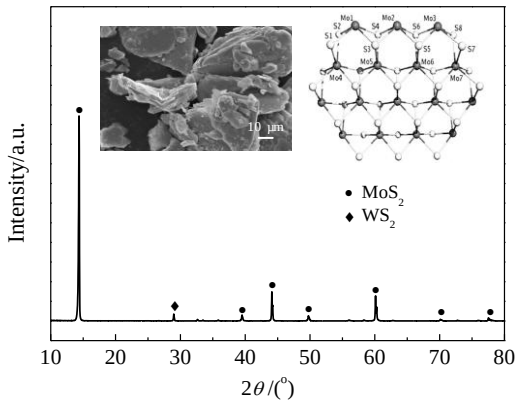

Fig.1 XRD pattern and SEM image of molybdenite

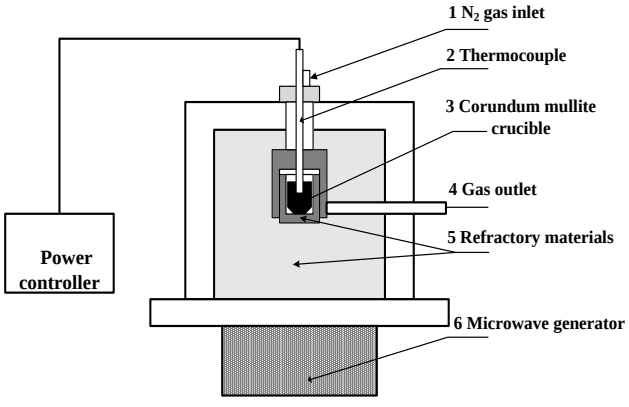

Fig.2 Schematic diagram of microwave activation equipment

2 Results and Discussion

2.1 Effect of microwave-activated pre-calcination

2.1.1 Irradiation power

The sulphur content of 30 g molybdenum calcine at 0, 0.4, 0.48, 0.56, and 0.64 kW is plotted in Fig.3. It can be seen that the sulphur content gradually decreases with increasing the microwave output power, and is far lower than that of sample M-0. Among them, the sulphur content of P-640 with microwave radiation power of 0.64 kW is 0.135%, and that of M-0 is relatively decreased by 65.47%.

Microwave heating has penetrability property. Energy absorbed by the material during the propagation of electromagnetic wave from the surface of the sample to the interior can be expressed by Eq.(1) [38],

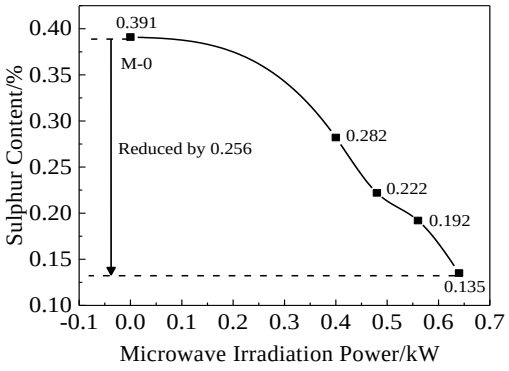

Fig.3 Sulphur content of molybdenum calcine versus microwave irradiation power

$$W = 2\pi f \varepsilon_0 \varepsilon'' \mathrm{tg}\delta |E|^2 V \quad (1)$$

where f, ε_0, ε'', tgδ, E and V represent the electromagnetic wave frequency, dielectric constant in vacuum, loss factor, tangent of dielectric loss, material internal electric field strength, and sample volume, respectively.

As can be seen from Eq.(1), when the electromagnetic wave frequency and the material volume are fixed, the microwave electric field intensity increases as the microwave output power increases, which is the direct energy absorption of the microwave material. Therefore the effect of the microwave activation on the pretreatment of the molybdenum calcine is even greater to significantly increase the reactivity and the oxidation degree of molybdenum in the subsequent oxidation roasting. The residual sulphur content of the molybdenum calcine sand can be reduced as a final result.

2.1.2 Material mass

The sulfur mass of 30, 50, 70, and 100 g molybdenite irradiated by 0.56 kW microwave power are plotted in Fig.4.

It can be seen that the sulphur content gradually increases with increasing the mass, and is far lower than that of sample M-0. Among them, the sulphur content of G-30 sample with a mass of 30 g is 0.192%, decreased by 50.8% compared to that of M-0.

In microwave field, the relationship between the material temperature increase rate and its mass is as follows [39]:

$$\frac{\mathrm{d}T}{\mathrm{d}\tau} = \frac{P}{\rho V c_\mathrm{p}} = \frac{2\pi f \varepsilon_0 \varepsilon'' E^2}{m c_\mathrm{p}} \quad (2)$$

where P and c_p represent the power obtained by absorbing materials per unit volume and specific heat capacity, respectively.

The material continuously absorbs microwave energy and then converts it into heat, which gradually attenuates the energy carried by the microwave. The penetration depth D_p of microwave in material is defined as the distance where the energy is the 1/e times of the original value to the surface after the microwave enters the material, which can be expressed by Eq.(3):

$$D_\mathrm{p} = \frac{\lambda_0}{2\pi\sqrt{2\varepsilon'}}\left[\sqrt{1+\left(\frac{\varepsilon''_\mathrm{eff}}{\varepsilon'}\right)}-1\right]^{-\frac{1}{2}} \quad (3)$$

where λ_0 is the electromagnetic wavelength in vacuum.

From Eq.(2, 3), it can be seen that the material volume increases with increasing mass, so does the attenuation of energy penetrating in microwave field, thereby weakening the microwave activation effect and temperature increase rate, and leading to an increase in residual sulphur, as shown in Fig.4.

2.1.3 Irradiation time

The sulfur mass of 30 g molybdenite irradiated by microwave power of 0.56 kW for 0, 3, 6, 9 and 12 min are plotted in Fig.5.

It can be seen that the sulphur content gradually decreases with prolonging the irradiation time, and is far lower than that of sample M-0. Among them, the sulphur content of sample T-12 after microwave-activated pre-calcination for 9 min is 0.156%, which is relatively decreased by 55.2% compared to inactivated sample M-0. This is because when the microwave output power and the material volume are fixed, the energy absorbed by the material is increased with the microwave radiation time, and the effect of microwave activation is enhanced, which leads to an increase in residual sulphur, as shown in Fig.5.

2.1.4 Structure and morphology change by microwave-activated pre-calcination

Specific surface area change versus microwave activation time and enlarged SEM images are shown in Fig.6 and Fig.7, respectively.

As can be seen from Fig.6 and Fig.7, the specific surface area of molybdenum calcine gradually increases with prolonging

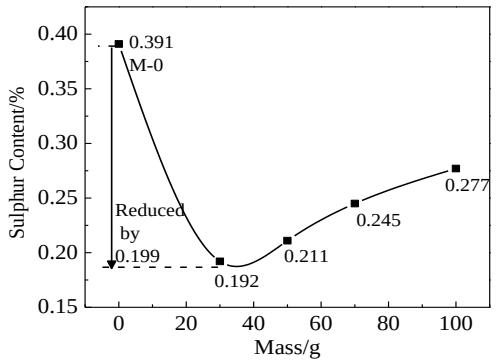

Fig.4 Sulphur content of molybdenum calcine versus sulphur mass

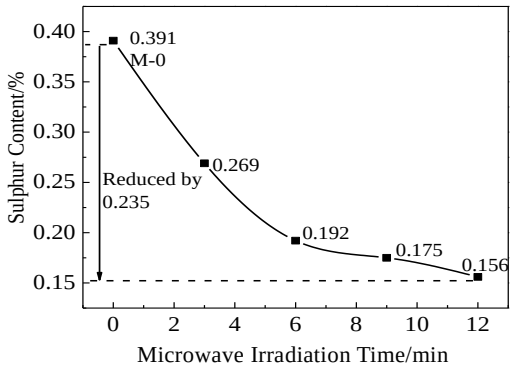

Fig.5 Sulphur content of molybdenum calcine versus microwave irradiation time

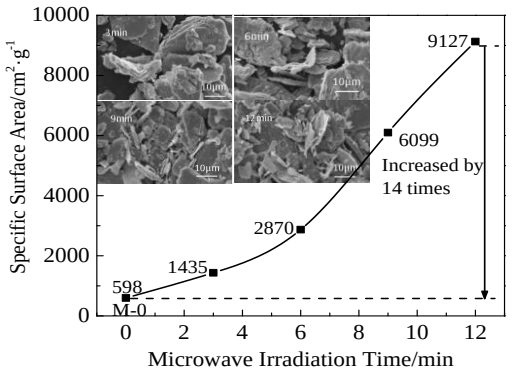

Fig.6 Effect of microwave activation time on specific surface area and surface morphologies of molybdenum calcine

the microwave-activated calcination time, and surface morphology of microwave activated molybdenum calcine becomes loose and porous and particle size changes obviously. In microwave field, MoS_2, as the main component of molybdenite, has a strong wave absorbing ability, which leads to a significant heating effect with high temperature rising rate (demonstrated further in the following part shown in Fig.9), while gangue components such as SiO_2 and CaO hardly absorb microwaves. Each component of molybdenite can be heated in a short time with different heating rates. Therefore, thermal stress between the internal components of molybdenite will be caused and when it reaches a certain level, interfacial cracks will appear between different components [40], and further crack propagation will promote the monomer dissociation of MoS_2, thereby increasing the specific surface area of molybdenite. As can be seen from Fig.6, the specific surface area of T-12 molybdenum calcine treated by microwave-activated pre-calcination for 12 min treated higher than that of M-0, with increase of 14.2 times. The lamellar structure of molybdenite is dissociated and more small-sized debris appear without external forces in microwave field. This means that microwave activation can improve the dynamic conditions of molybdenite oxidation roasting process.

From Fig.7, it can be seen that the microwave activation does not change the layered structure of the molybdenite itself, because of the hexagonal plate shape and extremely complete dissociation surface structure of molybdenite which enable the surface sliding when it is subjected to external forces [41]. Further changes of structure rarely happen because the connection between the layers is very strong Van der Waals forces rather than chemical bond. As a result, the size of lamellar structure of molybdenum calcine decreases when it is exposed to microwave radiation, and more scaly structure appears on the surface without minor appearance change but dynamic condition is improved.

The comparison of the (002) and (008) crystal surface peaks of the molybdenum calcine of microwave activated and inactivated samples is shown in Fig.8. The lattice constant, average grain size and microscopic strain of samples are shown in Table 2.

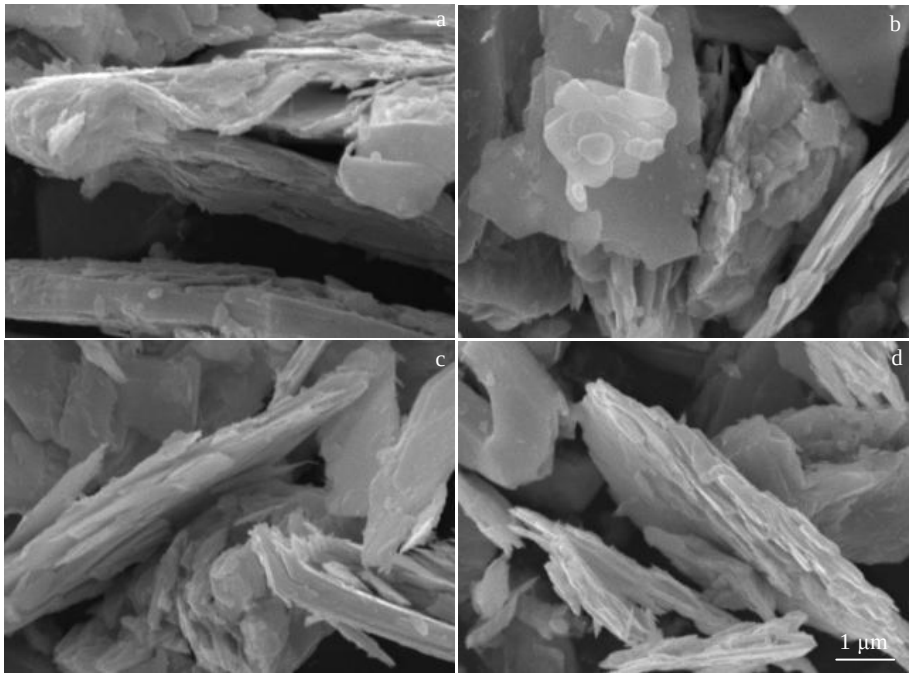

Fig.7 Enlarged SEM image of microwave activated molybdenum calcine for 0 min (a), 3 min (b), 6 min (c), and 9 min (d)

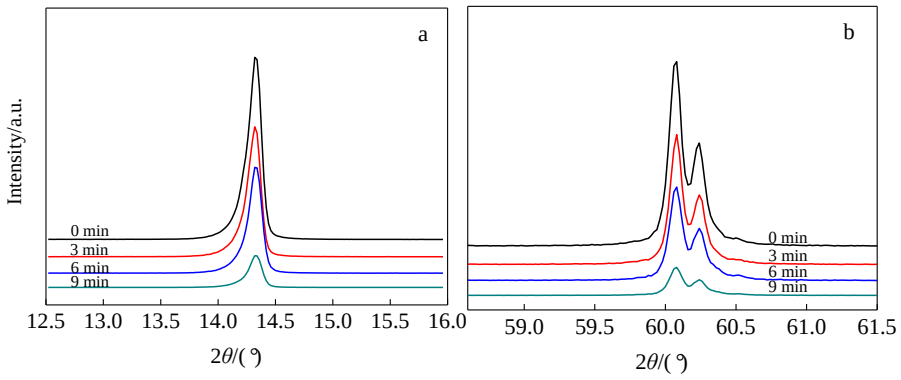

Fig.8 XRD patters of (002) (a) and (008) (b) crystal plane of samples with different irradiation time

Table 2 Lattice constant, average grain size and microscopic strain of molybdenum ore before and after microwave activation

Irradiation time/min	$a=b$/nm	c/nm	$\alpha=\beta$/(°)	γ/(°)	Lattice volume/nm^3	D/nm	ε/%
0	0.31659	1.23142	90	120	0.10689	86.9	0
3	0.31646	1.23156	90	120	0.10681	79.1	0.104
6	0.31644	1.23055	90	120	0.10672	74.0	0.119
9	0.31640	1.22947	90	120	0.10662	72.4	0.148

As can be seen from Fig.8, with the extension of the microwave activation time, the area surrounded by the (002) crystal plane peak and the (008) crystal plane peak of the molybdenite gradually decreases. Moreover, the intense energy released by microwave radiation impacts molybdenite in a short time, and it results in a lattice distortion of MoS_2, which is the main component of molybdenite. From Table 2, it can be seen that the values of a, b, and c of MoS_2 slightly decrease, the corresponding unit cell volume and crystallite size decrease, and the microscopic strain slightly increases with prolonging the microwave activation time. The dissociation effect and activation effect of microwave on molybdenite are illustrated.

2.2 Temperature rising characteristic of molybdenite in microwave field

The temperature rise characteristic of 40 g molybdenite in a microwave field of 0.56 kW is shown in Fig.9. The whole process can be divided into four stages according to the change of the heating rate shown in Table 3.

It can be seen that molybdenite has a rapid heating rate in the microwave field compared with in conventional heating equipment, and the temperature of the material increases significantly with prolonging the radiation time.

As for molybdenite, where MoS_2 exists as a main component, since the anion S^{2-} has a large ionic radius, it is easily polarized by other cations. When combined with other metal cations to form a mineral, they are easily polarized and thus the minerals and compounds containing Mo^{4+} have a faster heating rate [42]. Macroscopically, the microwave absorbing ability of MoS_2 is much stronger than that of

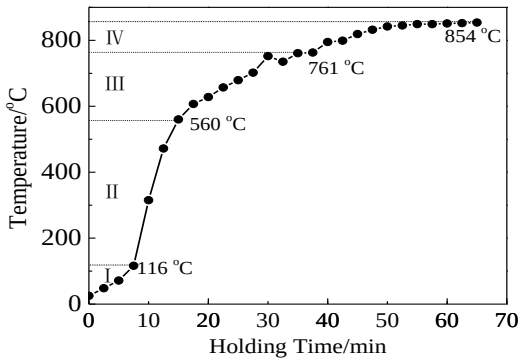

Fig.9 Temperature rise characteristic in microwave field

gangue, so local temperature difference and thermal stress will appear under microwave irradiation conditions, which will be beneficial for the dissociation of minerals and further increase the reaction area of MoS_2 involved in the oxidation reaction. In addition, the dissociation of minerals and the occurrence of cracks are beneficial to the escape of the product SO_2, which improves the oxidation effect and reduces the residual sulfur content of the final molybdenum oxide product.

2.3 Mass loss characteristics of molybdenite in microwave field

TG curve of molybdenite of microwave activated and inactivated sample with a heating rate of 5 ℃/min and an oxygen concentration of 20% is shown in Fig.10.

Table 3 Temperature rise stage of molybdenite

Stage	Temperature range/ ℃	Heating rate/ ℃·min^{-1}	Major feature description
Ⅰ	RT~116	12.1	Material drying and dissociation
Ⅱ	~560	59.2	Dramatic temperature increase reaches the oxidation reaction temperature and emitting heat: $2MoS_2(s)+7O_2=2MoO_3(s)+4SO_2(g)+995.1J$
Ⅲ	~761	10.0	Stable temperature rise and continuous oxidation stage
Ⅳ	~850	3.1	Stable heat preservation stage

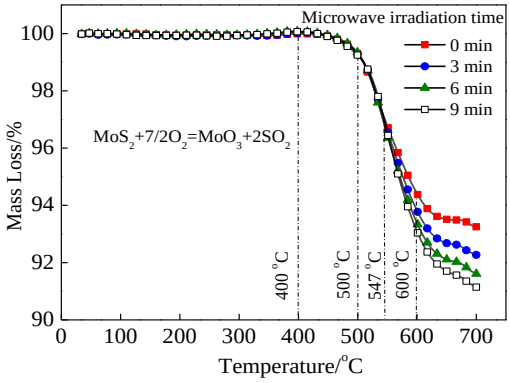

Fig.10 TG curves of molybdenite

It can be seen that the peak temperature of the TG curve is almost unaffected by microwave-activated pre-calcination, and is lower than 450 ℃, and four curves with different microwave activation time are basically overlapped; when oxidation reaction begins especially after heating up to the rapid oxidation stage (stage II in Fig.9 and Table 3), the microwave-activated effect is evident, and obvious differences of mass loss can be seen in Fig.10. When the temperature exceeds 500 ℃, the mass loss rate of molybdenite and slope of TG curve increase with prolonging the microwave pretreatment time (i.e., MoS_2 is continuously converted into MoO_3 during this stage), which indicates that the reaction speed of microwave activated molybdenum calcine roasting is significantly faster than that of conventional roasting.

In microwave field, the phenomenon of molecular polarization causes free energy exchange between microwave radiation energy absorbed by the molecule and its average kinetic energy, which results in a decrease in the activation energy of the reaction and a faster reaction rate; at the same time, the microwave has a higher vibration frequency, and it is likely to be close to the natural vibration frequency of the heating body molecule or the inherent vibration frequency of the chemical bond, which may cause the breaking

Table 4 Standard Gibbs free energy and reaction equilibrium constant for molar reaction of molybdenite oxidation roasting

T/ ℃	ΔG/kJ·mol^{-1}	K
300	−950.67	4.64×10^{86}
350	−939.16	5.57×10^{78}
400	−927.63	1.00×10^{72}
450	−916.09	1.54×10^{66}
500	−904.51	1.33×10^{61}
550	−892.97	4.76×10^{56}
600	−881.39	5.48×10^{52}
650	−869.86	1.69×10^{49}

of different chemical bonds in the molecule when the microwave causes vibration of the molecule, thereby increasing the reactivity[43-47]. After the activation pretreatment, the specific surface area and the microscopic strain of the molybdenum calcine increase, the average grain size decreases, and the surface morphology becomes looser, which effectively increases the reaction area with oxygen and improves the reaction kinetics, so the reaction rate and the desulfurization effect are significantly improved as a final result.

3 Thermodynamic and Reaction Kinetic Analysis

3.1 Roasting thermodynamic analysis

The reaction of microwave oxidation roasting of molybdenite, standard Gibbs free energy and chemical reaction equilibrium constant (K) can be described by Eq.(4~7). The standard molar reaction Gibbs free energy and chemical reaction equilibrium constant of the reaction at 300~650 ℃ can be calculated and are shown in Table 4.

$$MoS_2(s)+3.5O_2(g)\rightarrow MoO_3(s)+2SO_2(g) \quad (4)$$

$$\Delta rG_T^0=4.18\times\begin{pmatrix}-256870+14.67T\lg T-5.4\times10^{-3}T^2\\+0.62\times10^{-6}T^3+13.87T\end{pmatrix} \quad (5)$$

$$\Delta rG_T^0=-RT\ln K \quad (6)$$

$$\ln K=-\frac{\Delta rH_m}{RT}+C \quad (7)$$

where R is the molar gas constant.

The chemical reaction equilibrium constant (K) of molybdenite oxidation roasting is large, and this reaction can be regarded as an irreversible reaction according to Table 4. A very large equilibrium constant ensures that this reaction proceeds smoothly with a small partial pressure of oxygen. According to Van't Hoff's isostatic equation shown in Eq.(7), the enthalpy change in the oxidation reaction of molybdenite can be calculated. Equilibrium constants at different temperatures are plotted as ln$K$ versus 1/T, as shown in Fig.11, and linear regression is performed using the least-squares method.

The ΔH_m of the oxidation reaction calculated from the slope of the straight line in the figure is –1048.5 kJ/mol, indicating that the oxidation of molybdenite is a strongly exothermic process.

3.2 Roasting reaction kinetic analysis

3.2.1 Effect of temperature on the oxidation rate

The molybdenite was calcined at temperatures of 350, 400, 450, 500, 540, 580, 600, and 630 ℃. The changes in the effective oxidation rates of molybdenite at different temperatures and time are shown in Fig.12.

It can be seen that the effective oxidation rate increases significantly with increasing the calcination temperature and calcination time, and its average increasing rate is 7% from 350 ℃ to 540 ℃; when the calcination temperature is increased from 540 ℃ to 580 ℃, the effective oxidation rate increases significantly. Taking roasting for 20 min as an example, the effective oxidation rate increases from 30% to 62% at temperature ranging from 540 ℃ to 580 ℃, and the increase rate of the effective oxidation rate is kept at 100% when continuously prolonging the calcination time; when the calcination temperature is increased from 600 ℃ to 630 ℃, the increase rate of the effective oxidation rate does not change much, from 62% to 65%, basically kept in a level of roasting for 20 min; after roasting for 50 min, the oxidation rate is 82%~92%, and with longer roasting time, the effective oxidation rate remains stable. In addition, it can also be seen from the figure that the effective oxidation rate changes significantly from 20 min to 80 min at each temperature, while the effective oxidation rate does not in crease significantly after 90 min and the effective oxidation rate of molybdenite at 350 ℃ to 500 ℃ is lower than at higher temperatures. The effective oxidation rate of molybdenite is only 44% when calcined at 500 ℃ for 120 min, while that is 91% and 92% when calcined at 580 ℃ for 120 min and 630 ℃ for 120 min, respectively.

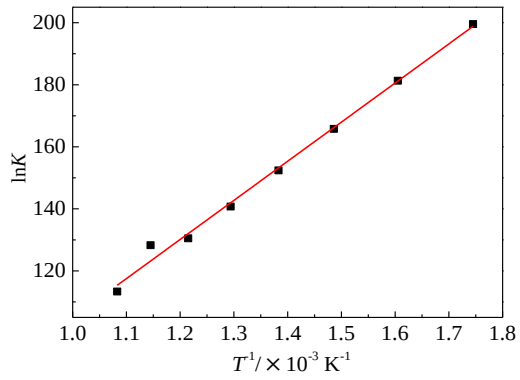

Fig.11 Relationship between ln$K$ and 1/T of molybdenite oxidation

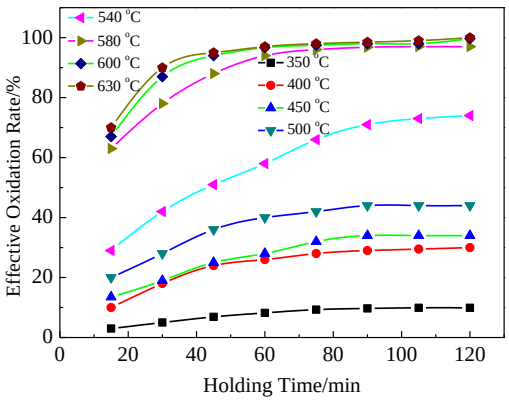

Fig.12 Effect of temperature and time on molybdenite oxidation efficiency

Cross-sectional SEM images of the oxide film of the molybdenite calcine at different temperatures are shown in Fig.13.

It can be seen that at lower reaction temperature (350, 400, 450, and 500 ℃), a dense oxidation products is observed on the molybdenum surface, which seriously impedes the diffusion of O_2 and SO_2, the effective oxidation and the final amount of residual sulphur. Morphology of oxidation product changes significantly to a slender and disperse form at temperature higher than 500 ℃, which is conducive to the improvement of the kinetics of the gas-solid reaction process, and the ultimate oxidation rate, and final effective oxidation rate increases. The SEM results are in good agreement with the results of the calcination experiment and consistent with the results in the Ref.[5].

3.2.2 Kinetic analysis of oxidation of molybdenite

Oxidized calcination can be regarded as a gas-solid reaction between solid molybdenite and oxygen. According to the unreacted nuclear model of gas-solid reaction shown in Fig.14, it can be seen [48] that oxide product will cover the molybdenite at reaction temperatures, hindering the diffusion of reactant O_2 and the escape of product SO_2. The oxidation process of molybdenite can be described as the following stages: (a) the mass transfer of oxygen to the surface of molybdenite to provide oxygen for the oxidation process; (b) the oxygen transfer under the molybdenite atomic force field and diffusion to the reaction interface by internal diffusion; (c) an interfacial chemical reaction of the adsorbed oxygen with molybdenite to form molybdenum oxide and SO_2; (d) product SO_2 transfer through the reaction interface and the solid phase product layer to the outside space by internal diffusion, external diffusion and mass transfer. The slowest stages of the above will be the rate controlling step of molybdenite oxidation process.

Assuming that molybdenite is a spherical particle with uniform particle size and surface activity, the size of the solid sample is hardly changed during the reaction. According to the gas-solid unreacted shrinkage nuclear model, when reaction is controlled by mass transfer (transfer of

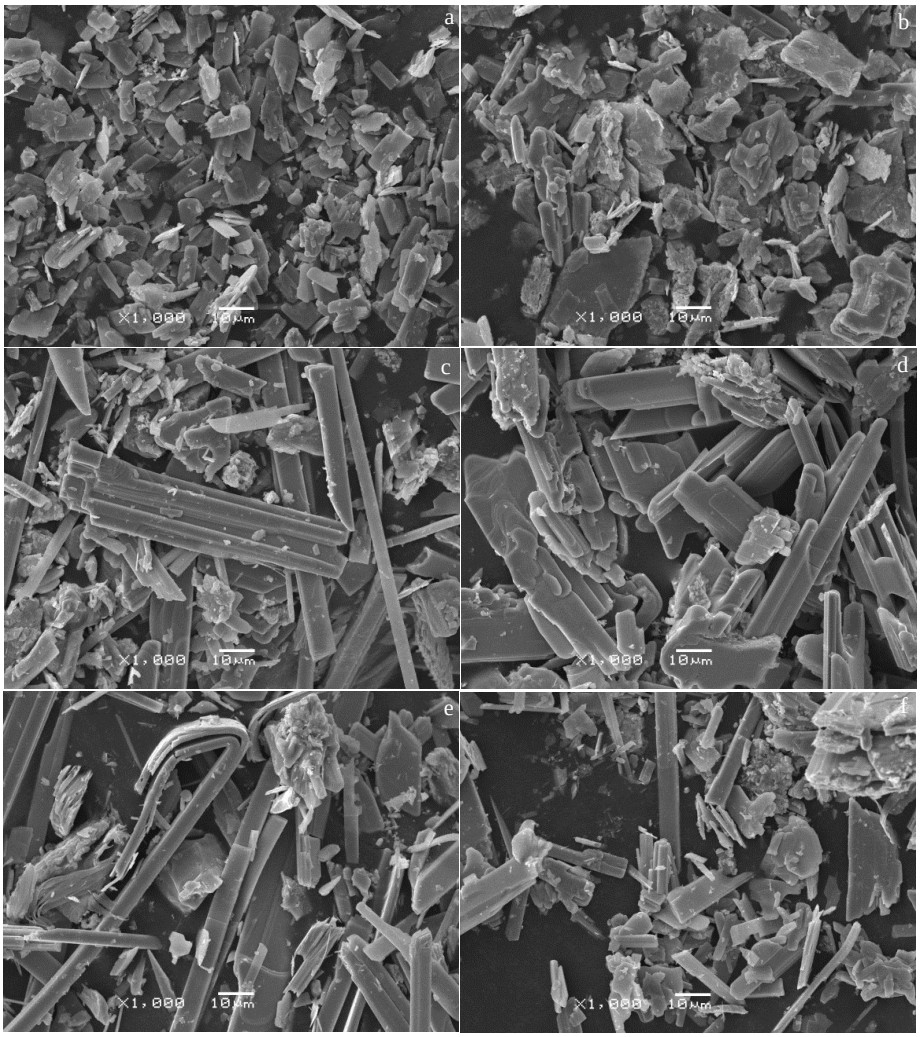

Fig.13 Morphologies of oxidation products of molybdenite at 450 ℃ (a), 500 ℃ (b), 540 ℃ (c), 580 ℃ (d), 600 ℃ (e), and 630 ℃ (f)

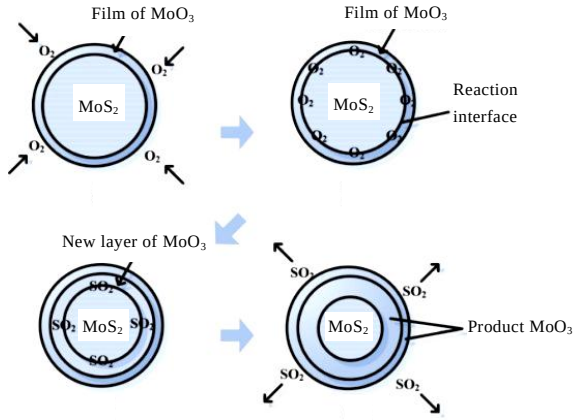

Fig.14 Schematic diagram of unreacted nuclear model of molybdenum oxidation process under microwave irradiation

gaseous reactants or products), interfacial chemical reactions, internal diffusion and out-diffusion, the effective oxidation rate and the oxidation time should satisfy the linear function of the characteristics shown in Eq.(8~11). So, the relationship of measured data and the linear function can be examined to tell the rate controlling step.

The effective oxidation rates of molybdenite at different temperatures were substituted into above four equations and plotted versus time, and the linear regression analysis was performed using the least squares method. Taking 450 and 540 ℃ as examples, the results are shown in Fig.15 and Fig.16, respectively.

$$F(x)=kt=x \quad (8)$$

$$F(x)=kt=1-(1-x)^{1/3} \quad (9)$$

$$F(x)=kt=1+2(1-x)-3(1-x)^{2/3} \quad (10)$$

$$F(x)=kt=x+(1-x)\ln(1-x) \quad (11)$$

From Fig.15a, the linear correlation coefficient between the characteristic function Eq.(10) and time t is the largest at 450 ℃, indicating that the oxidation process of molybdenite is controlled by internal diffusion at 450 ℃. From Fig.15b, the linear correlation coefficient between the characteristic function Eq.(9) and time t at 540 ℃ is the largest,

which indicates that the molybdenite oxidation process is controlled by the interface chemical reaction at 540 ℃.

Similarly, the correlation coefficient of each characteristic equation at different temperatures can be obtained. The linear correlation coefficient of the characteristic function Eq.(10) is bigger than that of Eq.(8, 9, 11) at 350 ℃ to 500 ℃, which indicates that the oxidation process of molybdenite at this stage is controlled by internal diffusion; the linear correlation coefficient of the characteristic function Eq.(9) is bigger than that of Eq.(8, 10, 11) at 540~630 ℃, which indicates that the oxidation process of molybdenite at this stage is controlled by the interface chemical reaction.

In order to obtain the kinetic parameters of molybdenite oxidation and to analyze the mechanism of oxidation reaction, the effective oxidation rate of molybdenite at 350~500 ℃ was substituted into the characteristic function Eq.(10) of the diffusion control model, and the effective oxidation rate of molybdenum at 540~630 ℃ was substituted into the characteristic function Eq.(9) of the interface chemical reaction control model. Results are shown in Fig.16 and Fig.17 by plotting characteristic function $F(x)$ against time t and the linear regression analysis of the characteristic function against time by the least square method.

From Fig.16 and Fig.17, it can be seen that the effective oxidation rate of molybdenite coincides with the calcination time in line and the linear relationship shown in Eq.(10) and Eq.(9) at 350~500 ℃ and 540~630 ℃, respectively. The apparent reaction rate constant k at different temperatures can be easily obtained from the slope of the straight line, as shown in Table 5. According to Table 5, the apparent reaction rate constant at 540~630 ℃ is ten times greater than that at 350~500 ℃, which means that with the increase of temperature, the mechanism of oxidation reaction of molybdenite is changed under the conditions of present study.

From the apparent rate constants at different temperatures shown above, and according to the Arrhenius equation Eq.(12), the apparent reaction activation energy of the molybdenite oxidation reaction controlled by internal diffusion and interface chemical reaction can be calculated.

$$\ln k = -\frac{E_a}{RT} + \ln A \tag{12}$$

where k, E_a, T and A represent the apparent reaction rate constant, apparent reaction activation energy, absolute temperature, and pre-factor, respectively.

The ln$k$ against 1/T at different temperatures was plotted, and linear regression was performed using the least squares method. The analysis results are shown in Fig.18 and Fig.19.

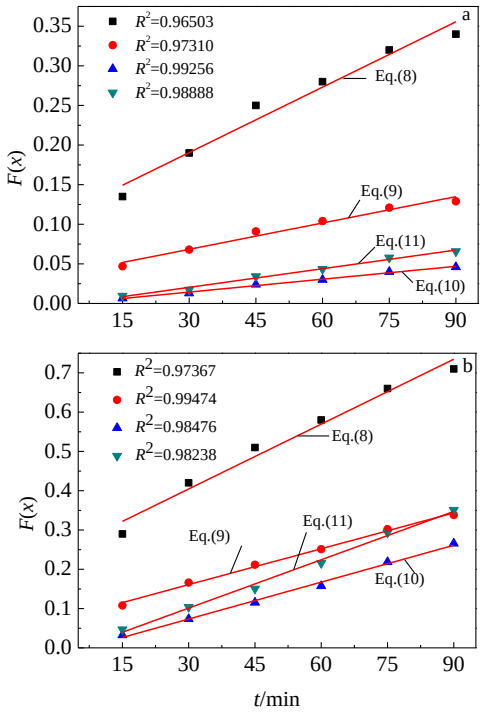

Fig.15 Relationship between $F(x)$ and t at 450 ℃ (a) 540 ℃ (b)

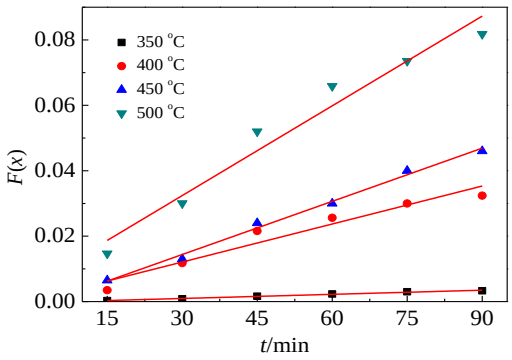

Fig.16 Relationship between $F(x)$ in Eq.(10) and time t at 350~500 ℃

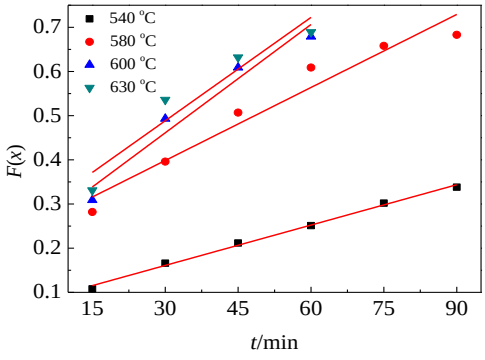

Fig.17 Relationship between $F(x)$ in Eq.(9) and time t at 540~630 ℃

According to the slope of the straight line in Fig.18 and Fig.19, the activation energy at 350~500 ℃ and 540~630 ℃ can be calculated to be 80.14 and 90.42 kJ/mol, respectively, which indicates the differences of reaction mechanism at the two temperature range.

Table 5 Reaction rate constants k at different temperatures

T/℃	k/×10^{-4} min	T/ ℃	k/×10^{-3} min
350	0.422	540	3.040
400	2.03	580	5.510
450	5.42	600	8.170
500	9.14	630	11.22

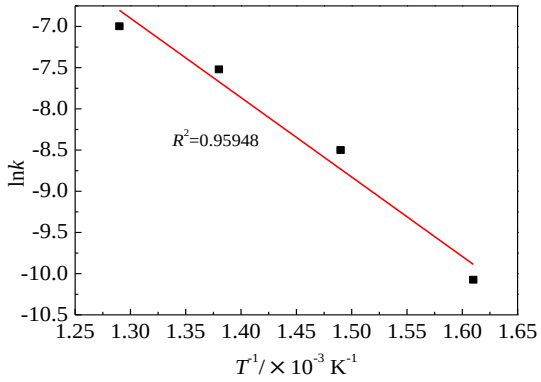

Fig.18 Arrhenius plot at 350~500 ℃

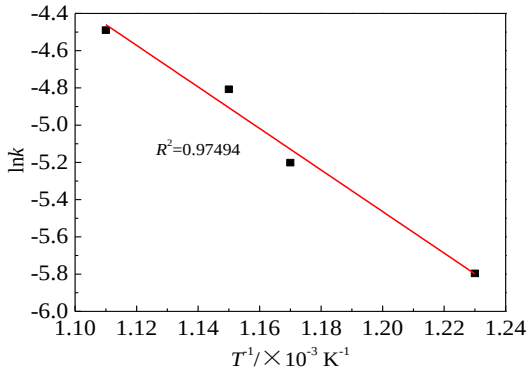

Fig.19 Arrhenius plot at 540~630 ℃

4 Conclusions

1) The microwave-activated pre-calcination treatment of molybdenite before conventional oxidative roasting is experimentally realized and verified. The optimal desulfurization effect can be obtained with microwave power of 0.64 kW irradiation on 30 g molybdenite for 6 min. The sulphur content is decreased by 65.47% relatively.

2) Microwave activation does not change the layered structure of the molybdenite itself but enhances the dissociation effect, which improves the dynamic conditions of molybdenite oxidation roasting process.

3) Microwave irradiation promotes the deep oxidation process at temperatures above 500 ℃ for oxidative roasting, accelerating the mass loss rate and reaction rate at this stage.

4) The molybdenite oxidation roasting is an irreversible strong exothermic reaction, so the higher the temperature, the faster the oxidation rate; the rate controlling factor for the roasting reaction at 350~500 ℃ is internal diffusion, and it is the chemical reaction rate at 540~630 ℃.

References

1 Lin C Y, Cheng X J. *Molybdenum ore Beneficiation and Deep Processing*[M]. Beijing: Metallurgical Industry Press: 1997: 13 (in Chinese)

2 Ma J, Zhang W Z. *Molybdenum ore Dressing*[M]. Beijing: Metallurgical Industry Press, 2008: 25 (in Chinese)

3 Guo P M, Wang D G, Zhao P. *Nonferrous Metals*[J], 2010(2): 6 (in Chinese)

4 Xiang T G. *Molybdenum Metallurgy*[M]. Changsha: Central South University Press, 2009 (in Chinese)

5 Zhang Q X, Zhao Q S. *Molybdenum Tungsten Metallurgy*[M]. Beijing: Metallurgical Industry Press, 2005: 26 (in Chinese)

6 Manoj K, Mankhand T R, Murthy D S R *et al. Hydrometallurgy*[J], 2007, 86(1-2): 56

7 Peng J R, Yang D J, Chen J X *et al. Chinese Journal of Rare Metals*[J], 2007, 31(6): 110 (in Chinese)

8 Ketcham J. *US Patent*, US6149883[P], 2000

9 Cao Z F, Zhong H, Liu G Y *et al. The Canadian Journal of Chemical Engineering*[J], 2009, 87(6): 939

10 Fu J G, Zhong H. *Journal of Central South University of Technology*[J], 2005, 12(2): 134

11 Cao Z f, Zhong H, Jiang T *et al. The Chinese Journal of Nonferrous Metals*[J], 2013, 23(8): 2290 (in Chinese)

12 Fu J G, Zhong H, Huang Y P *et al. Journal of Central South University of Technology, Natural Science*[J], 2004, 35(5): 797 (in Chinese)

13 Warren I H, Mounsey D M. *Hydrometallurgy*[J], 1983, 10(3): 343

14 Antonjevic M, Pacovic N V. *Minerals Engineering*[J], 1992, 5(2): 223

15 Romano P, Blazquez M L, Alguacilb F J *et al. FEMS Microbilology Letters*[J], 2001, 196(1): 71

16 Olson G J, Clark T R. *Hydrometallurgy*[J], 2008, 93(1-2): 10

17 Chen Jie, Li Dianjun, Liu Dachujn *et al. Gansu Metallurgy*[J], 2009, 31(1): 25 (in Chinese)

18 Gong Y B, Shen Y J, Ding Y *et al. Mining and Metallurgy Engineering*[J], 2009, 29(1): 78 (in Chinese)

19 Zou Zhenqiu, Zhou Qinjian. *Minning and Metallurgy Engineering*[J], 2002, 22(1): 79 (in Chinese)

20 Wang J F, Ding Z H, Zhang W J *et al. China Molybdenum Industry*[J], 1992(5): 15 (in Chinese)
21 Manoj G, Wong W L, Eugene. *Microwaves and Metals*[M]. New Jersey: John Wiley and Sons (Asia) Ltd, 2007
22 Yi J H, Tang X W, Luo S D *et al. Powder Metallurgy Technology*[J], 2003, 21(6): 351 (in Chinese)
23 Liang Liwei, Li Qiuling, Zeng Qingquan *et al. Hydrometallurgy of China*[J], 2011(1): 24 (in Chinese)
24 Osqjchuk J M. *IEEE Transactions on Microwave Theory & Techniques*[J], 1984, 32(9):1200
25 Guo G Z, Deng G Y, Tang H Y *et al. Journal of Henan University of Science & Technology*[J], 2014, 35(4): 5 (in Chinese)
26 Chen X Y, Zhou J W, Liu B G *et al. Inorganic Chemicals Industry*[J], 2015, 47(7): 12 (in Chinese)
27 Yang Kun, Zhu Hongbo, Peng Jinhui *et al. Mining & Metallurgical Engineering*[J], 2014, 23(5): 39 (in Chinese)
28 Zheng Qin, Zhang Libo, Peng Jinhui *et al. Mining & Metallurgy*[J], 2013, 22(4): 67 (in Chinese)
29 Chen J, Zhu H B, Peng J H *et al. Mining & Metallurgy*[J], 2014, 23(4): 83 (in Chinese)
30 Guo Lei, Zhang Libo, Peng Jinhui *et al. Mining & Metallurgy*[J], 2012, 21(4): 54 (in Chinese)
31 Wei Chenlong, Xu Lei, Zhang Libo *et al. Mining & Metallurgy*[J], 2016, 25(1): 31 (in Chinese)
32 Li Jie, Han Tengfei, Li Baowei *et al. Mining & Metallurgical Engineering*[J], 2014, 34(1): 82 (in Chinese)
33 Li Baowei, Han Lei, Li Jie *et al. Mining & Metallurgical Engineering* [J], 2015, 35(5): 99 (in Chinese)
34 Yu Qing, Ding Dexin, Zhang Ju *et al. Gold Science and Technology*[J], 2017, 25(1): 112 (in Chinese)
35 Guo S Q. *Study of Microwave Activated Roasting of Molybdenite*[D]. Xi'an: Xi'an University of Architecture and Technology, 2017 (in Chinese)
36 Hai Yulin. *China Molybdenum Industry*[J], 1984(1): 61 (in Chinese)
37 Ke Jiajun. *The Chinese Journal of Process Engineering*[J], 1981(4): 37 (in Chinese)
38 Zhou Jian, Cheng Jiping, Fu Wenrui *et al. Journal of Wuhan University of Technology*[J], 1999, 21(4): 4 (in Chinese)
39 Zhang Libo, Ma Aiyun, Peng Jinhui *et al. Transactions of Nonferrous Metals Society of China*[J], 2014, 24(12): 4004
40 Wei Li, Jia Wei. *Gold*[J], 24(12): 29 (in Chinese)
41 Shi W J, Zhang E G, Wang Z Y *et al. Journal of Shenyang Architectural & Civil Engineering Institute*[J], 2000, 16(1): 62 (in Chinese)
42 Jin Q H. *Microwave Chemistry*[M]. Beijing: Science Press, 2001 (in Chinese)
43 Chen Jin, Li Ning, Wang Shebin *et al. Journal of University of Science and Technology Beijing*[J], 2007, 29(9): 880 (in Chinese)
44 Cui Huijun, Chen Jin, Liu Jinying *et al. Journal of Iron and Steel Research*[J], 2007,19(11): 5 (in Chinese)
45 Luo Jun, Cai Chen, Lv Chunxu. *Chinese Journal of Synthetic Chemistry*[J], 2002, 10(1): 17 (in Chinese)
46 Zhou Xuiping, Yan Liuming. *Journal of Fuel Chemistry & Technology*[J], 1998, 26(6): 506 (in Chinese)
47 Zhang Hualian, Hu Ximing, Lai Shengli. *Journal of South China University of Technology, Natural Science*[J], 1997, 25(9): 46 (in Chinese)
48 Sun K. *Macroscopic Reaction Kinetics and Its Analytical Method*[M]. Beijing: Metallurgical Industry Press, 1998 (in Chinese)

微波活化焙烧辉钼矿生产低硫氧化钼

王　苗[1,2]，杨双平[1,2]，郭栓全[1]，曹栓伟[1]，何　凯[3]
(1. 西安建筑科技大学，陕西 西安 710055)
(2. 陕西省冶金工程技术研究中心，陕西 西安 710055)
(3. 金堆城钼业股份有限公司，陕西 西安 710077)

摘　要：对比研究了微波功率、作用时间及物料质量对辉钼矿预活化焙烧后的脱硫效果的影响，并采用气-固多相反应的未反应收缩核模型研究了辉钼矿氧化焙烧的动力学。结果表明，辉钼矿的吸波性能良好，在微波功率0.64 kW、物料质量30 g、微波作用6 min的条件下，微波可比常规处理方式显著降低硫含量0.256%；辉钼矿氧化焙烧是强放热反应，温度越高，辉钼矿氧化速率越快；540~630 ℃时转化率明显增高，界面化学反应是控制性环节。微波对于辉钼矿在常规氧化焙烧之前的活化作用已得到试验验证，若应用于工业生产，可采用短时间活化焙烧预处理来辅助常规的氧化焙烧。

关键词：辉钼矿；微波活化；预活化焙烧；低硫氧化钼；未反应核模型

作者简介：王　苗，女，1984 年生，博士，讲师，西安建筑科技大学陕西省冶金工程技术研究中心，陕西　西安　710055，电话：029-82202923，E-mail: wmxauat@163.com